

# Study of wake meandering by means of fixed point lidar measurements: Spectral analysis of line-of-sight wind component

**Davide Trabucchi, Gerald Steinfeld, David Bastine, Juan-José Trujillo, Jörg Schneemann and Martin Kühn**

ForWind-University of Oldenburg, Institute of Physics, Ammerländer Heerstr. 136, 26129 Oldenburg

E-mail: [davide.trabucchi@uni-oldenburg.de](mailto:davide.trabucchi@uni-oldenburg.de)

**Abstract.** The validation of dynamic wake meandering models by full field measurements is an important but challenging task. Recently a new approach has been proposed, where a long range lidar was employed to analyse the power spectral density of the line of sight wind component measured across the wake trajectory. The method is promising, but the number of useful time series within a measurement campaign depends to a large extent on a favourable geometrical setup of the lidar position and the wind direction. In the first part of the paper the approach is further investigated. To this avail, lidar simulations based on large eddy simulation results are analysed. In the second part, the approach is applied to real measurement data from a campaign with a long range lidar windscanner in the offshore wind farm »alpha ventus«. Eventually results about the wake dynamics are discussed.

## 1. Introduction

When a wind turbine is operating, it extracts energy from the wind passing through its rotor. In this process a wind deficit is generated which slowly recovers while it moves downstream. The area of the wind field affected by the wind deficit with increased local turbulence is commonly known as wake.

In a wind farm wind turbines often operate in the wake of other turbines. In these conditions, not only is the available energy of the wind less than in the free stream, but more severe turbulent fluctuations affect the turbine. A precise knowledge of the turbulence properties of the wake is therefore necessary to correctly predict the dynamic loading of the turbine structure in the design process. Hence, for instance, longer life-cycle or optimised structure design can derive from the reduction of the uncertainty on turbulence fluctuations in wakes.

The wake models applied in aero-elastic simulations can be divided in steady and dynamic models. The former consider a straight propagation of the wake where turbulence fluctuations are given by the combination of ambient and aero-dynamic turbulence [1]. The latter describe the wake as a series of deficit disks released at the turbine rotor and moving downstream transported by the atmospheric turbulent structures with scales larger than the rotor diameter [2; 3]. In these models the contribution of the so-called wake meandering, i.e. the lateral displacement of the wake deficit from the rotor axis, is taken into account along with the ambient and aero-dynamic turbulence.



A wind tunnel can be a suitable facility to study the dynamics of the wake [4; 5]. Synthetic wind fields generated by means of Large Eddy Simulation (LES) have been also applied to investigate the wake meandering [6; 7]. Nacelle based lidar have been implemented in full field experiments, for instance in [8; 9], to track dynamically the position of the wake center and to compare the results with the expectations from meandering models.

According to wake meandering models, the points near the lateral edges of the deficit are alternately inside and outside the wake. This results in a fluctuation of the wind component aligned with the rotor axis which is related to the wake dynamics. An approach to characterize the described fluctuations is proposed in [10], where long range lidar measurements are performed staring the laser beam at about hub height, diagonally across the wake. With this configuration, the necessity of an inclination about the axial wind direction has the drawback that only the wind turbulent fluctuations aligned with the lidar line of sight (LOS) can be measured. This aspect is investigated in the first part of this paper by means of lidar simulations, where a varying offset is applied between the LOS and the wind direction. In the central part, spectral characteristics of the LOS measurements previously simulated are evaluated for the study of the wake meandering. Eventually, fixed point lidar measurements collected in the offshore wind farm »alpha ventus« are considered. In particular, the power spectral density (PSD) of the data sampled across the wake of a wind turbine is analyzed.

## 2. Influence of the lidar beam inclination on the power spectral density of line of sight measurements

### 2.1. Lidar simulations

An unsteady, three dimensional wind field generated by the LES implementation PALM [11] is used as virtual environment for lidar simulations. The wake of a 2 MW Tjaereborg wind turbine with a rotor diameter  $D_T$  of 62 m and a hub height of 61 m is simulated by means of an actuator line (ACL) model [12]. The resulting wind field has a spatial and temporal resolution of 4 m and 0.4 s respectively.

The target of the lidar simulations was a point located at hub height in the wake of the described turbine, about  $3 D_T$  downstream with a lateral offset from the rotor axis of about 1 rotor radius  $R_T$ . The measurements were simulated with a 0.4 s sampling time. Four different LOS inclinations from the mean wind direction were considered, namely from  $0^\circ$  to  $60^\circ$  with a  $20^\circ$  increment. The layout of the simulations is illustrated in figure 1. In order to only estimate the influence of projection of the wind vector on the LOS direction, the volume average of the lidar measurements was not applied to the lidar simulations.

### 2.2. The PSD of the LOS wind component across the wake

The PSD of the simulated LOS measurements was evaluated by means of the Welch algorithm, applying 90 % overlapping rectangular windows of about 3 min duration and is presented in

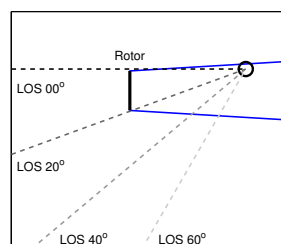


**Figure 1.** Layout of the lidar simulations (top view)

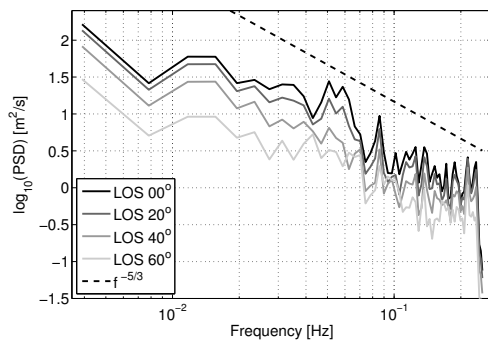


**Figure 2.** Power spectral density of the simulated LOS wind speed.

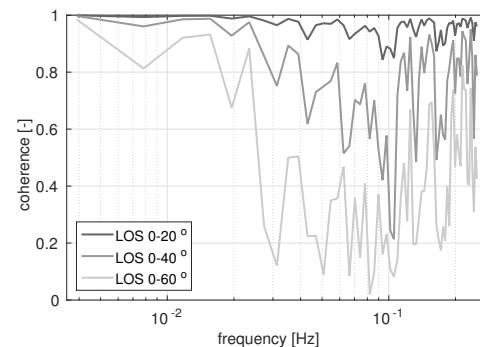


**Figure 3.** Variation of the spectral coherence between the simulated LOS measurements for an increasing angle of misalignment

figure 2. The 95 % confidence level conservatively estimated for this settings according to [13] corresponds to the range from  $-36\%$  to  $+79\%$  of the PSD value. From the graph it is evident that the energy content captured by the LOS projection decreases when the inclination angle increases. The spectral coherence function (SCF) can help to better interpret the results from the PSD analysis. It represents the normalized cross-spectral density between two signals [14] and indicates how well their spectral content is correlated. In particular, the SCF is constant and equal to 1 or 0 if the two considered signals are linearly correlated or completely uncorrelated. The SCF of the LOS simulated measurements aligned with the wind direction in relation to the ones with an increasing offset is depicted on the graph of figure 3. A coherence close to one is found for a deviation angle of  $20^\circ$ . For larger deviations a coherence value above 0.8 characterizes only the low frequency region, up to 0.02 – 0.03 Hz. Then it progressively decays and eventually starts fluctuating randomly. This result indicates that for long time fluctuations the vertical and transverse wind components are only weakly affecting the LOS projection even for larger direction offset.

### 3. Application of fixed point lidar measurements to the study of the wake meandering

A wake tracking procedure [8] has been applied to the wind field at the cross-section  $3 D_T$  downstream. The corresponding PSD of the lateral displacement of the wake deficit was evaluated to better understand whether a hidden relation exists between the lateral wake meandering and the fluctuations of the longitudinal wind speed at the lateral edge of the wake deficit. The normalized PSD of the wake lateral displacement and the one of the LOS measurements simulated with no offset with respect to the wind direction are compared in figure 4.

In both PSD curves, the energy is concentrated in the low frequency band and, at about 0.02 Hz, it starts decaying with a rate of about  $-5/3$ . While the PSD of the LOS simulations does not present any slope change in the high frequency range, the one of the wake lateral displacement sharply drops down. This may result from a low-pass filtering effect implicit in the wake-tracking procedure. Furthermore, the position of the wake center is supposed to be driven by the large-scale turbulent structures of the atmosphere.

It could be speculated on a resemblance to spectral peaks in the PSD of the LOS simulations near to 0.05 Hz and 0.09 Hz. This signature is not found in the spectral analysis of the wake tracking data, therefore no link with the wake meandering can be asserted. To better understand the nature of these possible peaks, further research will deal with longer datasets which could

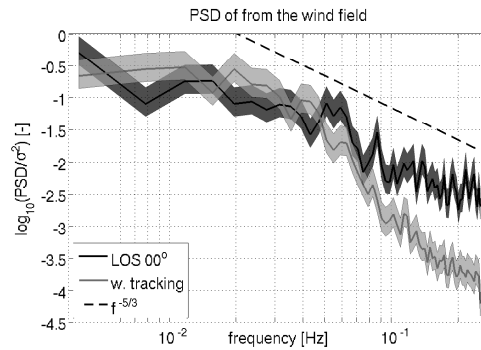


**Figure 4.** Normalized power spectral density and corresponding 95 % confidence level of the LOS simulations aligned with the wind direction and of the displacement of the wake center.

improve the statistical significance of the PSD.

#### 4. Offshore lidar measurements of the wake meandering

Three long range scanning lidars Windcube WLS200S were deployed at the offshore wind farm »alpha ventus« in the German North Sea for one year from spring 2013. Twelve 5 MW wind turbines from two different manufacturers are installed as illustrated in figure 5 from West to East in rows of four units. The six turbines in the northern half of the wind farm are characterized by a rotor diameter  $D$  of 126 m mounted on a 92 m high tower, while the six in the southern half have a 116 m rotor at an hub height of 90 m. Two lidars were positioned on the platform of the meteorological mast FINO1, while the third unit was installed on the transformer station AV0 near the south-east corner of the wind farm.

**Table 1.** Technical sheet of the Windcube WLS200S.

Properties		Acquisition	
Wave length	1.54 $\mu\text{m}$	Photodiode sampling rate	250 MHz
Pulse length (FWHM)	0.1 – 0.4 $\mu\text{s}$	FFT length	64 – 128 – 256 points
Max laser power	5 mW	LOS component accuracy	0.2 m/s
Pulse repetition rate	10 – 20 kHz	max # range gates	250
Max range	6500 m		

**Table 2.** Measurement setup.

Setting	Value
Azimuth angle	$-17.62^\circ$
Elevation angle	$1.80^\circ$
Pulse length (Full Width Half Maximum)	0.20 $\mu\text{s}$
FFT points	64
Accumulation/Sampling time	0.60 s
Physical resolution in line of sight	$\sim 40$ m

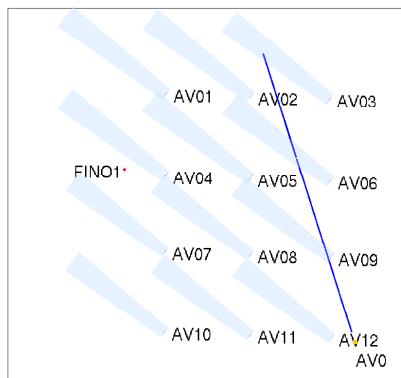


**Figure 5.** Position of the measurement beam (blue line) of the lidar installed on the transformer platform AV0 in the wind farm »alpha ventus«. Wakes are drawn downstream the turbines AV01-AV12 for a wind direction of  $127^\circ$ .

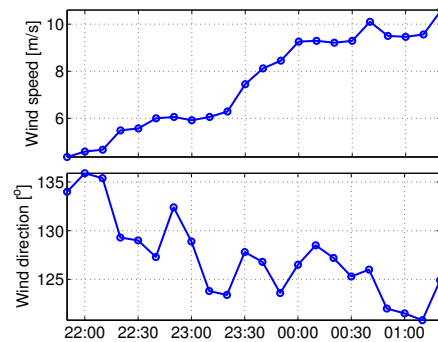


**Figure 6.** Ten-minute wind speed (top panel) and direction (bottom panel) collected by the top cup anemometer and the vane installed on the FINO1 meteorological mast at 100 m and 90 m respectively.

#### 4.1. Measurement setup

Staring lidar measurements were performed with the lidar installed on the transformer station. The target point was located at hub height in the middle position among the four turbines in the north-east corner of the wind farm. The 244 range gates implemented in this experimental campaign were distributed equally every 15 m between 100 m and 2992 m. A finer separation of 5 m was applied along a  $3 D$  distance centered to the aimed point. The objective of the measurements was to study the wake dynamics of the wind turbine AV06 by means of spectral analysis. The layout of the measurement is sketched in figure 5 for a wind direction of  $127^\circ$ , while the technical data and settings applied on the lidar are summarized in tables 1 and 2.

#### 4.2. Dataset description

The measurements took place for about 3 hours on 17/12/2013 at night. The ten minute average of the wind speed and direction measured during the campaign by the top cup anemometer and the wind vane installed on FINO1 at 100 m and 90 m respectively [15] is reported in figure 6. Figure 7 shows the full dataset of measurements. The wake of the wind turbines AV06 and AV09 are clearly visible within the shorter and further ranges respectively. Since only the measurements which took place in the wake of AV06 are at about hub height, only the further ranges were considered. Among all the data, only six ten minute intervals were analysed for this study. For sake of concision only the interval measured on 18/12/2013 at 01:04 is presented here. Data with a carrier to noise ratio (CNR) below  $-25$  dB or higher than  $-5$  dB was filtered out. Before the analysis, also outliers identified with the Chauvenet criterion [16] were excluded from the filtered time series. The remaining data was re-sampled applying a linear interpolation with a constant time step of 0.6 s.

In order to represent the LOS measurements in the fixed frame of reference of the wake of AV06, the orientation of the wake axis was determined using the center of the average deficit measured by the lidar. The derived wind direction, i.e.  $127^\circ$ , has a  $6^\circ$  offset with respect to the wind direction provided by the FINO1 instrumentation. The fact that for this direction FINO1 is in the wake of the wind farm could explain this deviation. In figures 8 and 9 the position of the measurement points along with the data considered in this study are represented in the

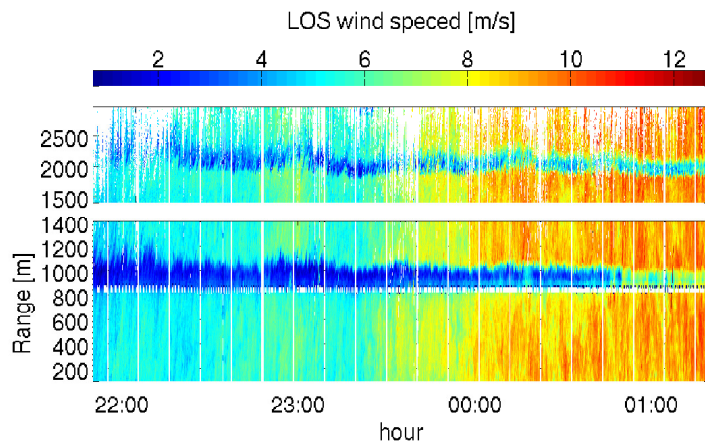


**Figure 7.** LOS measurements conducted on 17/12/2013 at night. In the top panel the measurements cross the wake of AV06, while in the bottom panel the one of AV09.

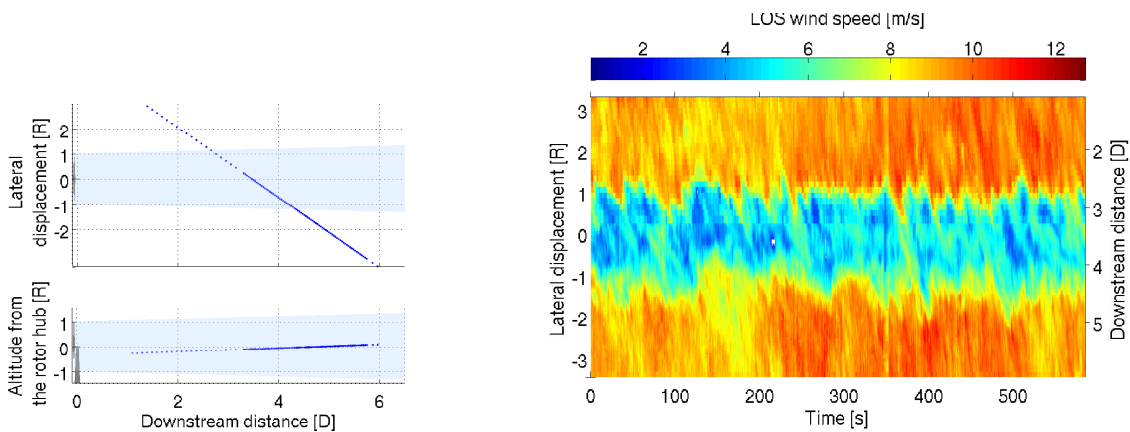


**Figure 8.** Top and side view of the measurement points represented in AV06 rotor frame of reference.

**Figure 9.** Ten minute time interval at 1:04 selected from the full dataset and represented in the AV06 rotor frame of reference.

reference frame of AV06 wake. Here, the  $x$  dimension is normalized with the rotor diameter  $D$ , while  $y$  and  $z$  with the corresponding radius  $R$ . Considering this setup, the inclination of the LOS from the wind direction is about  $35^\circ$ , which is an acceptable value according to the results of section 2.2.

#### 4.3. Spectral analysis

The PSD of the lidar measurements was performed applying the same procedure described in section 2.2. The related results are illustrated in figure 10 where the lateral boundaries of the wake can be easily identified. In fact, in this region the energy content is particularly high in relation to other positions over the rotor, especially in the low frequency range. Around  $2.7 D$  downstream, the area characterized by a higher level of the spectral energy covers a range of  $\pm 0.5 R$  across the edge of the wake. At the opposite edge, about  $4 D$  downstream, the range characterized by the increased PSD is almost twice as wide. This results are in accordance with [10], where a similar behaviour has been observed between  $1.5 D$  and  $4 D$  downstream. Figure 11 offers a closer view of the PSD of the LOS measurements evaluated at the center of

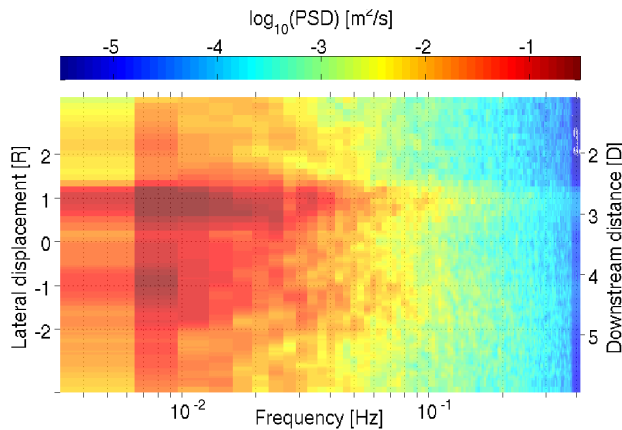


**Figure 10.** Power spectral density of the LOS wind component as a function of the frequency (abscissa), of the lateral displacement (left ordinate) and of the downstream position (right ordinate).

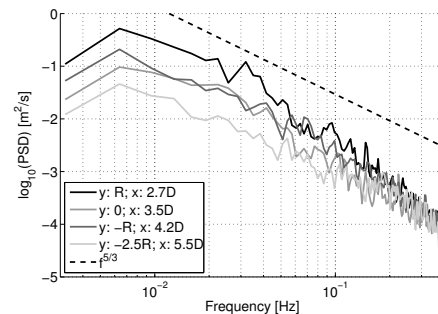


**Figure 11.** Power spectral density of the LOS wind component measured at different downstream distances, respectively at the lateral edges of the wake, in its center and in the free stream.

the wake  $3.5 D$  downstream and at the two opposite sides of the wake located at  $2.7 D$  and  $4.2 D$  respectively. The same graphic includes the PSD calculated in the free stream.

A comparison of the curves confirms that the spectral energy content outside the wake is remarkably lower than in the area affected by it. Moreover, the diagram reveals that the PSD values in the center and at the edge of the deficit are very similar in the far wake, while they are considerably higher in the transition between the near and far wake. The high spectral energy content found in the near wake at the boundary of the deficit seems to spread radially towards the center of the wake and towards the free stream while moving downstream, until eventually a quite uniform and lower level of turbulent energy is reached.

Considering the wake meandering models, these effect could be in part related to the amplitude of the displacement of the wake deficit, which generates the alternation of the measurement point position between in and outside the wake. In the transition between near and far wake smaller horizontal displacements characterize the wake due to the short time characterized by lateral transport, while, further downstream, the displacements could be larger than  $1 R$  as observed also in [17].

However, the increase of low frequency turbulence at the wake lateral boundaries could also be explained by turbulent diffusion. Only if an anti-correlation was found between the fluctuations measured at opposite sides of the wake, the relation between the fluctuations of the measurements at the edge of the wake and the wake meandering could be confirmed [5]. The applied measurement setup does not allow to perform the anti-correlation analysis for two points at the same downstream distance. The cross-correlation coefficient [14] has therefore been evaluated for the LOS time series sampled at the opposite edges of the wake deficit, but  $2.8 D$  and  $4.2 D$  downstream, respectively. The resulting curve visible in figure 12 as a function of the imposed time lag between the considered signals shows a minimum of  $-0.34$  for a time lag of 26 s. The corresponding peak is not necessarily statistically significant, for this reason a moderate anti-correlation can only be assumed. This hypothesis is sustained by the delay which is in the order of the expected travelling time of the deficit between the two considered points.

A dominant peak was probably not found because of the large longitudinal distance between the two considered points. To support this explanation, the cross-correlation analysis was applied

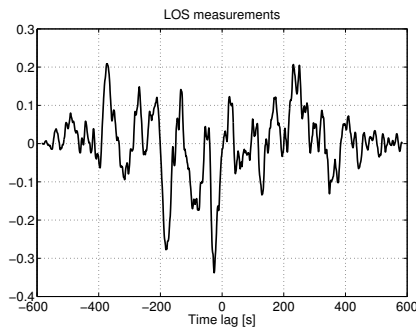


**Figure 12.** Cross-correlation of two LOS time series measured around hub height, at the opposite edges of AV06 wake deficit  $2.8 D$  and  $4.2 D$  downstream, respectively.

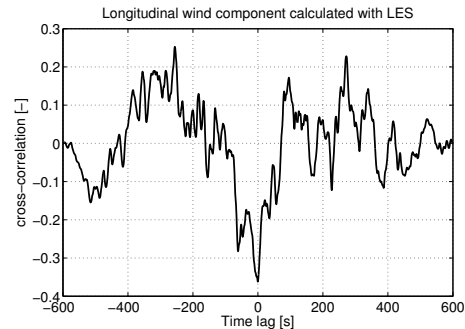


**Figure 13.** Cross-correlation of the longitudinal wind component sampled from the simulated wake of section 2.1 at hub height, at the opposite edges of the wake deficit, about  $3 D$  downstream, respectively.

with no downstream offset to the longitudinal wind component of the simulated wind field described in section 2.1. Two points at hub height, about  $3 D_T$  downstream and at opposite sides of the wake were considered. The related graph shown in figure 13 presents a clear evolution of the cross-correlation in which a negative peak and no time lag can be identified. This suggests that the results of the cross-correlation analysis from the full field lidar measurements could be improved if two points at the same downstream section were considered. Moreover, it indicates that the negative correlation found for the LOS measurements in figure 12 could be a real feature of the wind field and not just the outcome of an uncorrelated time series. For this reasons, a connection between the higher turbulence energy content at the edge of the wake and the wake meandering can be supposed.

## 5. Conclusion

In the first part of this work, simulations of lidar measurements at a fixed position in the wake of a wind turbine have been analysed to understand the influence of the misalignment between the LOS direction and the mean wind direction on the spectral analysis of the lidar measurements. It was demonstrated that LOS measurements at a fixed point can well represent the dynamic fluctuations of the main wind component at the edge of a wake deficit when they are oriented with a moderate offset with respect to the mean wind direction. The results suggest also that this constraint could be relaxed if only low-frequency fluctuations are considered.

To investigate the suitability of fixed point lidar measurements to the study of wake meandering, the normalized PSD of the lateral displacement of the wake center was compared with the one calculated for the LOS measurements simulated with no deviation from the wind direction. In both cases, the energy content mainly distributed within the low frequency range and then decays following a power law. No corresponding spectral peaks could be identified.

In the last part of the paper, full field data were considered. The measurement approach implemented in the simulations was reproduced in the offshore wind farm »alpha ventus« during an experimental campaign. In relation to other positions in the wake, a high level of spectral energy characterizes a well defined region around the lateral edges of the deficit in the transition between near and far wake. The meandering of the wake was suggested as possible explanation and a negative correlation between LOS measurements or simulations at opposite sides of the wakes supports this argument.

Fixed point lidar measurements showed to be a potential application for the study of the wake

dynamics by means of spectral analysis. This preliminary study indicates a possible relation between the wake meandering and the spectral characteristics of appropriate lidar measurements at the lateral boundaries of the wake. However, this hypothesis has to be confirmed by further research.

### Acknowledgments

The authors thank the whole »Lidar and Wakes« group at ForWind - University of Oldenburg which made the measurement campaign possible.

The research in the offshore wind farm »alpha ventus» was carried out in the frame of the RAVE (Research at alpha ventus) research project »GW Wakes - Part A«, funded by the German Federal Ministry for Economic Affairs and Energy (BMWi) based on a decision of the Parliament of the Federal Republic of Germany (grant number 0325397A).

### References

- [1] Frandsen S T and Thøgersen M 1999 *Wind Engineering* **23** 327–339 ISSN 0309-524X
- [2] Larsen G C, Madsen H A, Thomsen K and Larsen T J 2008 *Wind Energy* **11** 377–395 ISSN 1099-1824 URL <http://dx.doi.org/10.1002/we.267>
- [3] Trujillo J J and Kühn M 2009 *European Wind Energy Conference (EWEC)*
- [4] Medici D and Alfredsson P H 2008 *Wind Energy* **11** 211–217 ISSN 1099-1824 URL <http://dx.doi.org/10.1002/we.247>
- [5] España G, Aubrun S, Loyer S and Devinant P 2012 *Journal of Wind Engineering and Industrial Aerodynamics* **101** 24 – 33 ISSN 0167-6105 URL <http://www.sciencedirect.com/science/article/pii/S0167610511002157>
- [6] de Mare M, Mann J, Churchfield Matthew J and Patton Edward G 2013 *EWEA Offshore*
- [7] Bastine D, Björn W, Matthias W and Joachim P 2014 *Journal of Physics: Conference Series* **524**
- [8] Trujillo J J, Bingöl F, Larsen G C, Mann J and Kühn M 2011 *Wind Energy* **14** 61–75 ISSN 1099-1824 URL <http://dx.doi.org/10.1002/we.402>
- [9] Machefaux E, Larsen G C, Troldborg N, Gaunaa M and Rettenmeier A 2014 *Wind Energy* ISSN 1099-1824 URL <http://dx.doi.org/10.1002/we.1805>
- [10] Trabucchi D, Trujillo J J, Bitter M and Kühn M 2014 *Meteorologische Zeitschrift* – URL <http://dx.doi.org/10.1127/metz/2014/0610>
- [11] Raasch S and Schröter M 2001 *Meteorologische Zeitschrift* **10** 363–372 URL <http://dx.doi.org/10.1127/0941-2948/2001/0010-0363>
- [12] Troldborg N, Sorensen J N and Mikkelsen R 2010 *Wind Energy* **13** 86–99 ISSN 1099-1824 URL <http://dx.doi.org/10.1002/we.345>
- [13] Manolakis D G, Ingle V K and Kogon S M 2000 *Statistical and Adaptive Signal Processing* (McGraw-Hill) chap 5
- [14] Bendat J and Piersol A 2000 *Random data analysis and measurement procedures* (Wiley Interscience)
- [15] Beeken A, Neumann T and Westerhellweg A 2008 *DEWEK*
- [16] Taylor John R 1997 *An introduction to error analysis* (University Science Books)
- [17] España G, Aubrun S, Loyer S and Devinant P 2011 *Wind Energy* **14** 923–937 ISSN 1099-1824 URL <http://dx.doi.org/10.1002/we.515>